Trade-offs between unitary and measurement induced spin squeezing in cavity QED

Diego Barberena, 1,2,* Anjun Chu, 1,2 James K. Thompson, 1 and Ana Maria Rey, 1,2 IJILA, NIST and Department of Physics, University of Colorado, Boulder, Colorado 80309, USA, 2 Center for Theory of Quantum Matter, University of Colorado, Boulder, Colorado 80309, USA

(Received 8 October 2023; accepted 31 May 2024; published 16 August 2024)

We study the combined effects of measurements and unitary evolution on the preparation of spin squeezing in an ensemble of atoms interacting with a single electromagnetic field mode inside a cavity. We derive simple criteria that determine the conditions at which measurement based entanglement generation overperforms unitary protocols. We include all relevant sources of decoherence and study both their effect on the optimal spin squeezing and the overall size of the measurement noise, which limits the dynamical range of quantum-enhanced phase measurements. Our conclusions are relevant for state-of-the-art atomic clocks that aim to operate below the standard quantum limit.

DOI: 10.1103/PhysRevResearch.6.L032037

Introduction. Within the field of quantum metrology [1,2], spin squeezed states [3,4] constitute a concrete example of a quantum-enhanced resource with near-term practical applications. Their ability to measure spin rotations with a sensitivity that surpasses the standard quantum limit (SQL), i.e., the fundamental limit on phase estimation achievable with N uncorrelated particles, provides the opportunity for practical metrological gain in, e.g., atomic clocks [5,6], magnetometers [7–9], and matter-wave interferometers [10–12]. Consequently, schemes for efficient spin squeezing preparation [3,13,14] and experimental demonstrations in a variety of quantum platforms [5,15–21] have attracted considerable attention.

Particularly promising strategies for the scalable generation of squeezing are provided by QED cavities, where a shared light field mediates all-to-all interactions among atoms inside of a cavity. When driven by an external laser, the resulting dispersive atomic response is nonlinear and can be interpreted as an infinite range unitary Ising interaction called one-axis-twisting (OAT) [3]. This is known to create spin squeezing [3] and this specific drive-induced mechanism is known as cavity-feedback squeezing [5,18,21,22]. On the other hand, after atoms and light interact, photons leaking out of the cavity carry information about the atomic ensemble [17,19,20] that can be accessed by continuously monitoring the output light via quantum nondemolition (QND) measurements [13,23,24]. Adequate use of this information allows for the estimation of the number of nonexcited atoms, which decreases the noise of the state along the magnetization axis, leading to spin squeezing.

In this paper we examine the possible advantages of combining both methods of preparation. We employ a general

Published by the American Physical Society under the terms of the Creative Commons Attribution 4.0 International license. Further distribution of this work must maintain attribution to the author(s) and the published article's title, journal citation, and DOI.

analytical framework, analogous but distinct to the ones presented in Refs. [25,26], that considers the effects of finite detection efficiency, and include from the outset fundamental sources of noise and dissipation.

Our main result can be stated succinctly: when the detection efficiency of the QND measurement is above 0.19, QND outperforms OAT. Otherwise, the choice between QND or OAT depends on other experimentally relevant parameters such as spin flip probability, cavity cooperativity, and atom number [see Fig. 4(c) for details]. We also perform a systematic study of the area of the generated measurement noise, which negatively impacts the dynamical range and utility of the state for quantum-enhanced phase measurements [27].

Model. We begin with a simple model that exemplifies the physics that we are trying to describe [28] [see Fig. 1(a)]. We consider an ensemble of N atoms with three levels: $|\uparrow\rangle$, $|\downarrow\rangle$, and $|e\rangle$ in the level configuration shown in Fig. 1(a). The excited state has a finite lifetime, and decays to $|\uparrow\rangle$ and $|\downarrow\rangle$ with rates γ_1 and γ_2 , respectively. The atoms interact with a single mode of a single port QED cavity, with resonance frequency ω_c , which is detuned from resonance with the $|\uparrow\rangle$, $|\downarrow\rangle \rightarrow |e\rangle$ transitions by $\pm \Delta$, as illustrated in Fig. 1(a). The cavity is in turn driven close to resonance by a laser tone at frequency ω_d [detuning $\delta = \omega_d - \omega_c$, see Fig. 1(a)] and input flux of $|\beta|^2$ photons per second, and the transitions $|\uparrow\rangle$, $|\downarrow\rangle \leftrightarrow |e\rangle$ are coupled to the cavity with single photon Rabi frequencies $2g_1$ and $2g_2$, respectively. The light that comes out of the system can then be measured in a homodyne configuration with detection efficiency η .

Under conditions (to be stated later) that permit adiabatic elimination of the excited state $|e\rangle$ and the cavity degree of freedom, the system evolves under an effective Ito stochastic differential equation [29,30]

$$d\hat{\rho} = \left\{ -i\chi \left[\hat{S}_{z}^{2}, \hat{\rho} \right] + \Gamma \mathcal{L}_{\hat{S}_{z}}(\hat{\rho}) + \frac{\gamma_{sc}}{2} \sum_{k=1}^{N} \left(\frac{(1-p)}{2} \mathcal{L}_{\hat{\sigma}_{z}^{k}}(\hat{\rho}) \right) \right.$$

^{*}Contact author: diego.barberena@colorado.edu

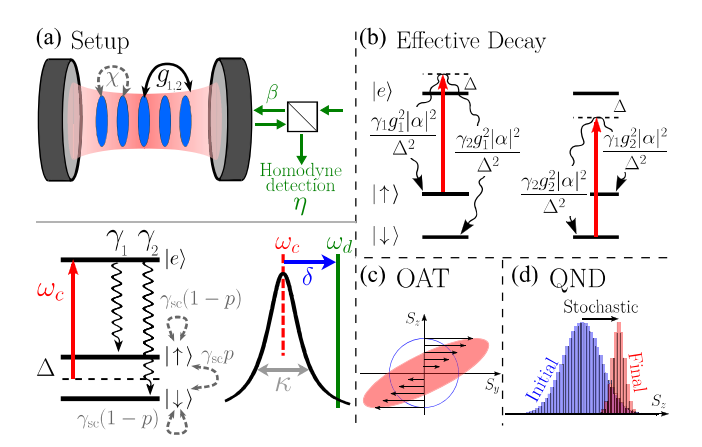


FIG. 1. (a) Schematic of the model: a three level system interacting with a QED cavity, which is in turn driven by a laser. Output light is measured via homodyne detection with efficiency η . Dashed gray lines represent effective processes (χ , γ_{sc}). (b) Effective single particle processes in ground manifold. (c) OAT dynamics shears the noise distribution, causing it to get squeezed. (d) Schematic of QND, showing pre (blue) and post (red) measurement distribution in the basis of \hat{S}_z .

$$+ p[\mathcal{L}_{\hat{\sigma}_{+}^{k}}(\hat{\rho}) + \mathcal{L}_{\hat{\sigma}_{-}^{k}}(\hat{\rho})] \bigg) \bigg\} dt$$
$$+ \sqrt{\Gamma \eta} (\hat{S}_{z}\hat{\rho} + \hat{\rho}\hat{S}_{z} - 2 \langle \hat{S}_{z} \rangle \hat{\rho}) dW, \tag{1}$$

where $\hat{S}_{x,y,z} = \sum_{k=1}^N \hat{\sigma}_{x,y,z}^k/2$ are collective spin operators acting on the ground manifold $|\uparrow\rangle$, $|\downarrow\rangle$, $\hat{\sigma}_{x,y,z}^k$ are Pauli matrices acting on atom k, and χ , Γ , γ_{sc} , p are effective parameters related to experimental quantities (precise definitions will be provided later). Unitary dynamics is described by the parameter χ . Incoherent evolution is expressed in terms of Lindbladians $\mathcal{L}_{\hat{L}}(\hat{\rho}) \equiv \hat{L}^{\dagger}\hat{\rho}\hat{L} - \{\hat{L}^{\dagger}\hat{L},\hat{\rho}\}/2$, and includes collective dephasing (Γ) and single particle spin conserving $[\gamma_{sc}(1-p)]$ and spin changing $(\gamma_{sc}p)$ incoherent processes. The final line of Eq. (1) incorporates continuous measurement of \hat{S}_z via homodyne detection (in an appropriately chosen quadrature) [30,31] with efficiency η , and includes a stochastic Wiener increment dW to model the probabilistic nature of quantum measurements. The output of the measurements is a time-dependent current $i(t) \equiv dq/dt = 2\sqrt{\Gamma\eta} \, \langle \hat{S}_z \rangle + dW/dt$.

To unpack the content of Eq. (1), we consider that all the atoms begin in the superposition $|\uparrow\rangle + |\downarrow\rangle$, which is relevant to experimental implementations and corresponds to a Bloch vector entirely polarized along the x direction, i.e., $\langle \hat{S}_x \rangle = N/2$. Furthermore, to obtain a manageable set of equations we use a large N approximation, in which the state remains gaussian, but relax these assumptions later. In this limit the Bloch vector remains polarized along x but relaxes due to γ_{sc} according to $\langle \hat{S}_x \rangle = N e^{-\gamma_{sc}t/2}/2$. Fluctuations perpendicular to the Bloch vector satisfy [29,32,33]

$$\begin{split} \dot{v}_{zz} &= -\Gamma \eta N v_{zz}^2 - 2 \gamma_{\text{sc}} p(v_{zz} - 1) \\ \dot{v}_{yy} &= 2 \chi N v_{zy} e^{-\gamma_{\text{sc}} t/2} + \Gamma N e^{-\gamma_{\text{sc}} t} - \Gamma N \eta v_{zy}^2 - \gamma_{\text{sc}} (v_{yy} - 1) \\ \dot{v}_{zy} &= \chi N e^{-\gamma_{\text{sc}} t/2} v_{zz} - \Gamma \eta N v_{zz} v_{zy} - \frac{\gamma_{\text{sc}}}{2} (2p + 1) v_{zy}, \end{split}$$
 (2

where $v_{ab} = (2 \langle \{\hat{S}_a, \hat{S}_b\} \rangle - 4 \langle \hat{S}_a \rangle \langle \hat{S}_b \rangle)/N$ (for a, b = z, y) are (co)variances normalized to the spin projection noise. The equation for v_{zz} ($\propto \hat{S}_z$ variance) evolves under two competing effects: measurements $(\Gamma N \eta)$ reveal information about the magnetization and thus reduce v_{77} [see Fig. 1(d)]. On the other hand, spin flips $(\gamma_{sc}p)$ restore the variance to its initial uncorrelated value $v_{zz} = 1$. For v_{yy} (\hat{S}_y variance), single particle processes (γ_{sc}) also restore the variance to its uncorrelated value, but measurement backaction (ΓN) instead increases the variance. Furthermore, coherent interactions (χN) mix v_{yy} with v_{zy} and leave v_{zz} untouched, reflecting the shearing dynamics characteristic of OAT [see Fig. 1(c)] that leads to a noise distribution squeezed along an intermediate direction in the \hat{S}_z/\hat{S}_v plane. Note that dW does not appear in these equations, indicating that the dynamics they describe does not depend on the specific measurement outcomes.

Measurements do introduce small stochastic corrections to the orientation of the Bloch vector that manifest as deflections in the yz plane. In a small time interval dt, these deflections satisfy [29]

$$dz = -\gamma_{sc} p z dt + \sqrt{\Gamma \eta N} v_{zz} dW$$

$$dy = (\chi N e^{-\gamma_{sc} t/2} z - \gamma_{sc} y/2) dt + \sqrt{\Gamma \eta N} v_{zy} dW, \quad (3)$$

where $z = \langle \hat{S}_z \rangle / \sqrt{N/4}$ and $y = \langle \hat{S}_y \rangle / \sqrt{N/4}$. The measured current evolves according to $dq = \sqrt{\Gamma N \eta} z dt + dW$ and is connected to y and z through the common increment dW. To take advantage of the measurement process these deflections need to be calculated accurately using i(t), since they are different for each measurement realization. Neglecting this information leads to an average state that is not squeezed in any directions.

The absolute scale for time is set by the total scattering rate from the excited state induced by the probe [see Fig. 1(b)] γ_{sc} :

$$\gamma_{\rm sc} = \frac{\gamma_1 g_1^2 |\alpha|^2}{\Lambda^2} + \frac{\gamma_1 g_2^2 |\alpha|^2}{\Lambda^2} + \frac{\gamma_2 g_1^2 |\alpha|^2}{\Lambda^2} + \frac{\gamma_2 g_2^2 |\alpha|^2}{\Lambda^2}, \quad (4)$$

where $|\alpha|^2 = \kappa |\beta|^2/(\delta_*^2 + \kappa^2/4)$ is the number of circulating photons in the cavity, found by multiplying the incident photon flux, $|\beta|^2$ [see Fig. 1(a)], by the cavity buildup factor $\kappa/(\delta_*^2 + \kappa^2/4)$, and $\delta_* = \delta - (g_1^2 - g_2^2)N/2\Delta$ is the detuning of the drive with respect to the dressed cavity mode. The other effective parameters can be expressed in terms of $\gamma_{\rm sc}$, $d = 2\delta_*/\kappa$ and $C = 4g_1^2/(\kappa\gamma_1) = 4g_2^2/(\kappa\gamma_2)$, the single particle cooperativity, which is a property of cavity geometry:

$$\chi = \frac{C\gamma_{\rm sc}d/2}{1+d^2}, \quad \Gamma = \frac{C\gamma_{\rm sc}}{1+d^2}, \quad p = \frac{2\gamma_1\gamma_2}{(\gamma_1+\gamma_2)^2} \leqslant \frac{1}{2}.$$
 (5)

The spin flip probability p measures the relative importance of single particle spin changing processes relative to spin conserving processes, both of which arise through virtual excitation of the excited state and subsequent decay into the ground manifold [see Fig. 1(b)].

Cavity feedback squeezing arises when $\delta_* \gg \kappa$. Then $\chi \gg \Gamma$ and OAT dominates until single particle processes disrupt the generation of spin squeezing. QND measurements operate in the opposite regime: $\delta_* = \chi = 0$ and Γ maximal. In the absence of γ_{sc} , the resulting evolution continuously projects the system onto an \hat{S}_z eigenstate, reducing the variance of \hat{S}_z even beyond the gaussian limit [see Fig. 1(d)]. However, the precise

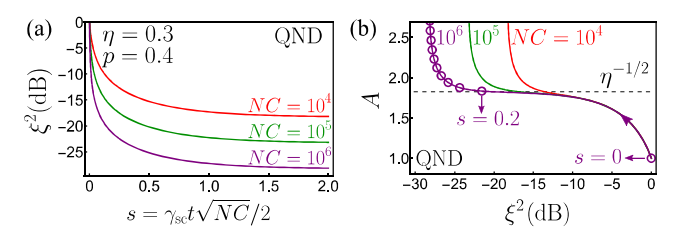


FIG. 2. (a) Squeezing (ξ^2) as a function of time for various NC in the QND configuration. (b) QND squeezing vs state area (A) plotted parametrically with time as a parameter. Circles are equally spaced in s intervals of size 0.2.

eigenstate onto which the system is projected is stochastic and must be estimated accurately using the measurement record.

Adiabatic elimination gives rise to Eq. (1) when $\Delta \gg \gamma_{1,2}, 2g_{1,2}|\alpha|, 2g_{1,2}\sqrt{N}$. These conditions guarantee that the excited state is never appreciably populated and that the atom-cavity interaction is dispersive.

Squeezing and state area. Equation (2) must be solved with initial conditions $v_{zz}(0) = v_{yy}(0) = 1$ and $v_{zy}(0) = 0$. Within the gaussian regime, the evolution generates a noise distribution on the yz plane in the form of a ellipse whose axes have minimum (maximum) length v_{\min} (v_{\max}) [29], and in terms of which we define

$$\xi^2 = e^{\gamma_{\rm sc}t} v_{\rm min}, \quad A = e^{\gamma_{\rm sc}t} \sqrt{v_{\rm min} v_{\rm max}}.$$
 (6)

The Wineland squeezing parameter ξ^2 [34] quantifies the metrological enhancement of phase measurements compared to uncorrelated atoms (SQL) and includes the effects of reduced contrast. The state area A measures the size of the noise distribution, normalized to the length of the Bloch vector squared. When $\gamma_{\rm sc}=0$ and $\eta=1$ then A remains of order 1, but loss of information leads to an area that can be substantially larger. An increase in A reduces the metrological utility of the generated squeezing since it limits the range of phases that can be measured with some degree of quantum enhancement [27].

Measurement limit. Here $\delta_* = \chi = 0$ and $\Gamma = C\gamma_{\rm sc}$. Assuming that $NC\eta \gg 1$, simple analytic solutions can be written for the fluctuations and the estimator of $\langle \hat{S}_z \rangle$ [29]. The minimum-variance axis lies along z, giving rise to a Wineland parameter of

$$\xi_t^2 = v_{zz} = \sqrt{\frac{2p}{NC\eta}},\tag{7}$$

within the timescale $\tau = (NC\eta p)^{-1/2}/(2\gamma_{\rm sc})$, while v_{yy} grows as $1 + NC\gamma_{\rm sc}t$ and $v_{zy} = 0$. The subscript t in ξ_t^2 indicates that ξ^2 has been optimized over time. ξ^2 is depicted as a function of $s = \gamma_{\rm sc}t\sqrt{NC}/2$ for different values of NC in Fig. 2(a).

Waiting for a few τ times gets ξ^2 closer to ξ_t^2 , but waiting for too long leads to uncontrolled growth of v_{yy} and hence of state area. We show this in Fig. 2(b), where we plot A vs ξ^2 parametrically as a function of time. The sharp upward turn in the curve indicates that A is growing without any improvement in ξ^2 . Notice also that there are plateaus of constant $A = \eta^{-1/2}$, more visible at larger NC. In these plateaus spin flips are not yet active, so the decrease in \hat{S}_z variance is exactly compensated by the increase in \hat{S}_y variance.

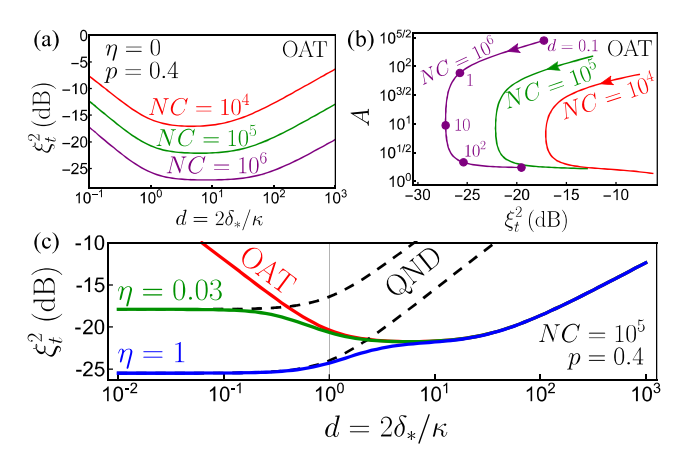


FIG. 3. (a) Time optimized squeezing (ξ_t^2) as a function of detuning in the OAT configuration for various NC. (b) OAT squeezing vs state area plotted parametrically using d as a parameter. Each filled circle occurs at a value of d ten times bigger than the previous one. (c) Squeezing optimized over time as a function of d at fixed p = 0.4 and $NC = 10^5$ for different η . Solid red is OAT ($\eta = 0$) and dashed black is pure QND (\hat{S}_τ variance).

Unitary limit. Here $\eta = 0$ and $\delta_* \gg \kappa$. Equation (2) is now linear and can be solved exactly, but we consider the effects of $\gamma_{\rm sc} p$ on ξ^2 perturbatively. Assuming $\chi Nt \gg 1$, this leads to [29,35]

$$\xi^2 \approx \frac{1}{\chi^2 N^2 t^2} + \frac{\Gamma/\chi}{\chi N t} + \frac{2}{3} \gamma_{\rm sc} p t. \tag{8}$$

The first and second terms include the effects of interactions (χ) and collective dephasing (Γ) , respectively. The third term is due to spin flips and is the main obstruction for unitary spin squeezing.

The behavior of ξ_t^2 (time optimized squeezing) with d depends on whether collective dephasing (Γ) is active at the optimal squeezing time or not. If Γ is active, relevant for smaller values of d, then ξ_t^2 arises from the competition between the second and third terms in Eq. (8), leading to $\xi_t^2 = \xi_{t,\delta}^2 \sqrt{1 + 1/d^2}$, where

$$\xi_{t,\delta}^2 = \sqrt{\frac{32p}{3NC}} \tag{9}$$

is the best possible squeezing attainable in this region, obtained roughly at $d \ge 1$. This leads to a very broad minimum in ξ_t^2 , depicted in Fig. 3(a) for various NC. This trend lasts until $d \approx 1.7(CN/p)^{1/4}$, after which Γ is no longer active, and ξ_t^2 now arises from the competition between the first and third terms in Eq. (8). Further increase in d worsens $\xi_t^2 \sim [pd/(NC)]^{2/3}$ (independent of κ) because interactions get smaller than the spin flip rate. The optimal squeezing is thus given by Eq. (9).

While the region of minimum ξ_t^2 is very broad in Fig. 3(a), the state area at each of these points is distinct. We show this in Fig. 3(b), where ξ_t^2 vs A is plotted parametrically using $d = 2\delta_*/\kappa$ as a parameter for various NC. The leftmost vertical sections of the curves indicate the optimal $\xi_{t,\delta}^2$, but the variation in A is quite dramatic. It is preferable to work at larger values of d, potentially sacrificing a few dB of ξ_t^2 in exchange for a substantially smaller area, as has been pointed out before [21,22].

Measurement and unitary evolution. Here we analyze whether a combination of measurements and unitary evolution, operating at some finite value of d for a given $\eta \neq 0$, can improve upon the two limiting situations described in the previous sections.

In Fig. 3(c) we show the results of simulating numerically Eq. (2), where at any given detuning d and η , squeezing has been optimized over time within a time window of $s \in [0, 50]$ (this accounts for the fact that at $\delta_* = 0$ the optimal is only reached asymptotically). From the curves shown for different η , it can be observed that ξ_t^2 is obtained either purely through measurements at $\delta_* = 0$ or in the unitary limit, where the value of η is irrelevant. Thus, the decision to use measurements vs OAT is determined by the comparison between Eqs. (7) and (9). They are equal when the efficiency η has the value

$$\eta_c \equiv \frac{3}{16} = 0.1875. \tag{10}$$

When $\eta > \eta_c$, measurements are efficient enough that operating at $\delta_* = 0$ is preferable. When $\eta < \eta_c$, unitary evolution will lead to a better ξ_r^2 .

Absence of spin flips. In cycling transitions p is very close to zero and the analysis based on Eq. (2) is no longer applicable because the state evolves beyond the Gaussian regime and gets distorted, thus introducing corrections (typically called "finite-size" or "curvature" effects) that limit the attainable spin squeezing. In the OAT setting ($\eta = 0$), this is remedied by solving Eq. (2) with p = 0 and adding an extra curvature term to the minimum variance [3,35,36],

$$\xi^2 \approx e^{\gamma_{\rm sc}t} \left(\frac{e^{\gamma_{\rm sc}t} + \Gamma N t}{\chi^2 N^2 t^2} + \frac{\chi^4 N^4 t^4}{6N^2} \right).$$
 (11)

A comparison with the analytical solution of Eq. (1) for p=0 indicates that Eq. (11) captures accurately the time optimized ξ^2 [29]. Variations of N or C now have different effects on ξ^2 , whereas previously they only appeared in the combination NC.

When p=0, the time optimized ξ_t^2 shows three distinct behaviours as a function of detuning, depicted in Fig. 4(a). For $d<2.3N^{1/3}$, collective dephasing is active, competes with the curvature term, and leads to $\xi_t^2\approx 2N^{-2/5}d^{-4/5}$ [36,37] and $A=1.76N^{1/5}/d^{3/5}$. When $2.3N^{1/3}< d<0.4CN^{2/3}$, the optimal squeezing arises from unitary dynamics, leading to the well-known OAT result $\xi_t^2=1.04N^{-2/3}$ [3] and $A=\sqrt{1.5}$, independent of d. For $d>0.4CN^{2/3}$, the exponential prefactors are the main obstruction to squeezing, and lead to $\xi_t^2\approx 6.8d^2/(N^2C^2)$ and $A\approx\sqrt{e}$. Furthermore, the existence of the OAT minimum imposes a restriction on the cooperativity: $C>6N^{-1/3}$. Otherwise, the center region in Fig. 4(a) disappears.

As p is increased, the dependence of ξ_t^2 on d will switch from the one in Fig. 4(a) to the one in Fig. 3(a) at some specific value p_{c_1} . We can estimate p_{c_1} by equating the exact OAT result and Eq. (9):

$$p_{c_1} = \frac{0.1C}{N^{1/3}}. (12)$$

In the QND setup (d=0) at p=0, the system will approach a state with no \hat{S}_z variance in a timescale $\sim (\Gamma \eta)^{-1}$, but squeezing will be limited by loss of contrast. This is shown in Fig. 4(b), which is obtained by solving semianalytically

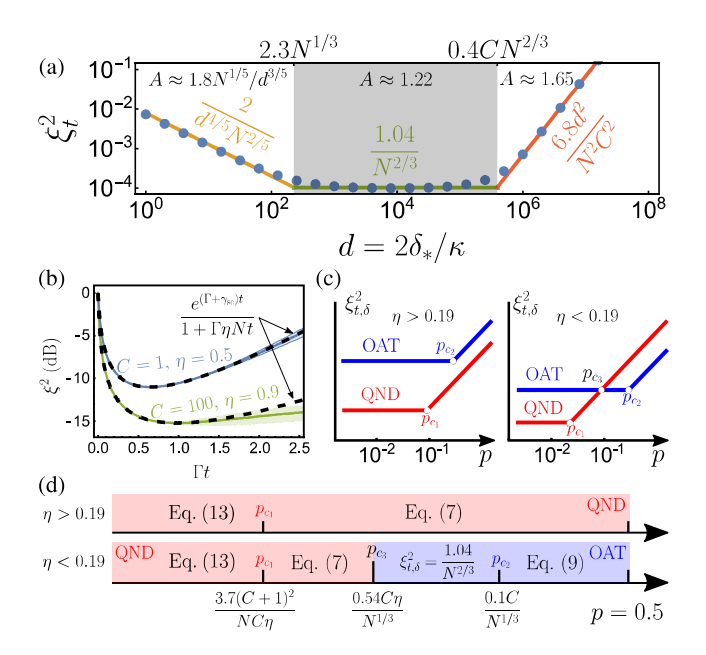


FIG. 4. (a) Time optimized spin squeezing ξ_t^2 as a function of d when p=0, $\eta=0$, $C=10^2$, and $N=10^6$. (b) Time profile of ξ^2 for two values of (η,C) averaged over measurement realizations. Shaded areas indicate the dispersion of ξ^2 values over different individual measurements. Dashed black is an analytical model, with $\Gamma=C\gamma_{\rm sc}$. (c) Optimal spin squeezing for OAT and QND as a function of p for different η . (d) Summary of results.

Eq. (1) [29] for p = d = 0, N = 100 and averaging ξ^2 over different measurement trajectories. At the optimal time, the average squeezing is

$$\xi_t^2 \approx \frac{e}{N\eta} \left(1 + \frac{1}{C} \right),\tag{13}$$

calculated using the model depicted in Fig. 4(b) [dashed black] [29], which captures reasonably well the dynamics of the average ξ^2 , though individual measurement trajectories may reach better values of ξ_t^2 when $C \gtrsim 1$ and $\eta \approx 1$ [see Fig 4(b), shaded area]. Equating Eqs. (13) and (7) indicates that this minimum can be reached when $p < p_{c_2} = e^2(C + 1)^2/(2NC\eta)$.

Summary and conclusions. These results form a coherent picture, summarized in terms of a few key statements, and shown schematically in Figs. 4(c) and 4(d).

(i) $\eta > 0.1875$: QND is better than OAT for any value of spin flip probability p.

(ii) $\eta < 0.1875$: OAT dominates over QND for p close to 1/2. As p is reduced OAT saturates to the curvature-limited ideal minimum, but QND continues to improve according to Eq. (7). QND will outperform OAT when $p < p_{c_3} = 0.54C\eta/N^{1/3}$ [obtained by equating Eq. (7) and the squeezing at the ideal OAT minimum] as long as $\eta > 2.6(1 + C^{-1})/N^{1/3}$ [obtained by equating Eq. (13) and the ideal OAT minimum]. Otherwise OAT ourperforms QND for all p (not depicted in Fig. 4).

In [29] we discuss how to use our results to set bounds on the achievable squeezing in experiments where our analysis applies [17–21,38]. Future research will involve analysis

of two-tone schemes [39], the consequences of parking the cavity closer to atomic resonance [21,33], comparisons with time-reversal based unitary protocols [28,40–42] and including more complicated unitary dynamics (e.g., twist and turn, two axis twisting) [43–45] using the stochastic equation formalism.

- Acknowledgments. We thank C. Luo and M. Miklos for a careful reading and comments on the manuscript. This material is based upon work supported by the VBFF, the National Science Foundation under Grants No. PFC PHY-2317149 (Physics Frontier Center) and No. OMA-2016244 (QLCI Q-SEnSE) and NIST.
- C. L. Degen, F. Reinhard, and P. Cappellaro, Quantum sensing, Rev. Mod. Phys. 89, 035002 (2017).
- [2] L. Pezzè, A. Smerzi, M. K. Oberthaler, R. Schmied, and P. Treutlein, Quantum metrology with nonclassical states of atomic ensembles, Rev. Mod. Phys. 90, 035005 (2018).
- [3] M. Kitagawa and M. Ueda, Squeezed spin states, Phys. Rev. A 47, 5138 (1993).
- [4] J. Ma, X. Wang, C. Sun, and F. Nori, Quantum spin squeezing, Phys. Rep. 509, 89 (2011).
- [5] E. Pedrozo-Peñafiel, S. Colombo, C. Shu, A. F. Adiyatullin, Z. Li, E. Mendez, B. Braverman, A. Kawasaki, D. Akamatsu, Y. Xiao, and V. Vuletić, Entanglement on an optical atomic-clock transition, Nature (London) 588, 414 (2020).
- [6] J. M. Robinson, M. Miklos, Y. M. Tso, C. J. Kennedy, T. Bothwell, D. Kedar, J. K. Thompson, and J. Ye, Direct comparison of two spin squeezed optical clocks below the quantum projection noise limit, Nat. Phys. 20, 208 (2024).
- [7] D. Budker and M. Romalis, Optical magnetometry, Nat. Phys. 3, 227 (2007).
- [8] T. Thiele, Y. Lin, M. O. Brown, and C. A. Regal, Self-calibrating vector atomic magnetometry through microwave polarization reconstruction, Phys. Rev. Lett. 121, 153202 (2018).
- [9] H. Zheng, Z. Sun, G. Chatzidrosos, C. Zhang, K. Nakamura, H. Sumiya, T. Ohshima, J. Isoya, J. Wrachtrup, A. Wickenbrock, and D. Budker, Microwave-free vector magnetometry with nitrogen-vacancy centers along a single axis in diamond, Phys. Rev. Appl. 13, 044023 (2020).
- [10] M. Kasevich and S. Chu, Atomic interferometry using stimulated Raman transitions, Phys. Rev. Lett. 67, 181 (1991).
- [11] A. D. Cronin, J. Schmiedmayer, and D. E. Pritchard, Optics and interferometry with atoms and molecules, Rev. Mod. Phys. 81, 1051 (2009).
- [12] G. P. Greve, C. Luo, B. Wu, and J. K. Thompson, Entanglementenhanced matter-wave interferometry in a high-finesse cavity, Nature (London) 610, 472 (2022).
- [13] A. Kuzmich, N. P. Bigelow, and L. Mandel, Atomic quantum non-demolition measurements and squeezing, Europhys. Lett. 42, 481 (1998).
- [14] W. Qin, Y.-H. Chen, X. Wang, A. Miranowicz, and F. Nori, Strong spin squeezing induced by weak squeezing of light inside a cavity, Nanophotonics **9**, 4853 (2020).
- [15] W. Muessel, H. Strobel, D. Linnemann, D. B. Hume, and M. K. Oberthaler, Scalable spin squeezing for quantum-enhanced magnetometry with Bose-Einstein condensates, Phys. Rev. Lett. 113, 103004 (2014).
- [16] J. G. Bohnet, B. C. Sawyer, J. W. Britton, M. L. Wall, A. M. Rey, M. Foss-Feig, and J. J. Bollinger, Quantum spin dynamics and entanglement generation with hundreds of trapped ions, Science 352, 1297 (2016).

- [17] M. H. Schleier-Smith, I. D. Leroux, and V. Vuletić, States of an ensemble of two-level atoms with reduced quantum uncertainty, Phys. Rev. Lett. 104, 073604 (2010).
- [18] I. D. Leroux, M. H. Schleier-Smith, and V. Vuletić, Implementation of cavity squeezing of a collective atomic spin, Phys. Rev. Lett. **104**, 073602 (2010).
- [19] K. C. Cox, G. P. Greve, J. M. Weiner, and J. K. Thompson, Deterministic squeezed states with collective measurements and feedback, Phys. Rev. Lett. 116, 093602 (2016).
- [20] O. Hosten, N. J. Engelsen, R. Krishnakumar, and M. A. Kasevich, Measurement noise 100 times lower than the quantum-projection limit using entangled atoms, Nature (London) 529, 505 (2016).
- [21] B. Braverman, A. Kawasaki, E. Pedrozo-Peñafiel, S. Colombo, C. Shu, Z. Li, E. Mendez, M. Yamoah, L. Salvi, D. Akamatsu, Y. Xiao, and V. Vuletić, Near-unitary spin squeezing in ¹⁷¹Yb, Phys. Rev. Lett. **122**, 223203 (2019).
- [22] Y.-L. Zhang, C.-L. Zou, X.-B. Zou, L. Jiang, and G.-C. Guo, Detuning-enhanced cavity spin squeezing, Phys. Rev. A 91, 033625 (2015).
- [23] V. B. Braginsky, Y. I. Vorontsov, and K. S. Thorne, Quantum nondemolition measurements, Science **209**, 547 (1980).
- [24] V. B. Braginsky and F. Y. Khalili, Quantum nondemolition measurements: the route from toys to tools, Rev. Mod. Phys. 68, 1 (1996).
- [25] Z. Li, B. Braverman, S. Colombo, C. Shu, A. Kawasaki, A. F. Adiyatullin, E. Pedrozo-Peñafiel, E. Mendez, and V. Vuletić, Collective spin-light and light-mediated spin-spin interactions in an optical cavity, PRX Quantum 3, 020308 (2022).
- [26] L. A. Fuderer, J. J. Hope, and S. A. Haine, Hybrid method of generating spin-squeezed states for quantum-enhanced atom interferometry, Phys. Rev. A 108, 043722 (2023).
- [27] B. Braverman, A. Kawasaki, and V. Vuletić, Impact of non-unitary spin squeezing on atomic clock performance, New J. Phys. 20, 103019 (2018).
- [28] E. Davis, G. Bentsen, and M. Schleier-Smith, Approaching the Heisenberg limit without single-particle detection, Phys. Rev. Lett. 116, 053601 (2016).
- [29] See Supplemental Material at http://link.aps.org/supplemental/10.1103/PhysRevResearch.6.L032037 for derivations of the atom-light model in Eq. (1)–(3), calculation of the bounds given in Eqs. (7), (9), (13), and an application of our results to a variety of experimental platforms.
- [30] H. M. Wiseman and G. J. Milburn, *Quantum Measurement and Control* (Cambridge University Press, Cambridge, 2009).
- [31] K. Jacobs and D. A. Steck, A straightforward introduction to continuous quantum measurement, Contemp. Phys. 47, 279 (2006).
- [32] L. B. Madsen and K. Mølmer, Spin squeezing and precision probing with light and samples of atoms in the Gaussian description, Phys. Rev. A 70, 052324 (2004).

- [33] Z. Zhang, Y. Zhang, H. Guo, L. Wang, G. Chen, C. Shan, and K. Mølmer, Stochastic mean-field theory for conditional spin squeezing by homodyne probing of atom-cavity photon dressed states, arXiv:2306.00868 [quant-ph].
- [34] D. J. Wineland, J. J. Bollinger, W. M. Itano, F. L. Moore, and D. J. Heinzen, Spin squeezing and reduced quantum noise in spectroscopy, Phys. Rev. A 46, R6797(R) (1992).
- [35] A. Chu, P. He, J. K. Thompson, and A. M. Rey, Quantum enhanced cavity QED interferometer with partially delocalized atoms in lattices, Phys. Rev. Lett. 127, 210401 (2021).
- [36] M. H. Schleier-Smith, I. D. Leroux, and V. Vuletić, Squeezing the collective spin of a dilute atomic ensemble by cavity feedback, Phys. Rev. A 81, 021804(R) (2010).
- [37] M. H. Schleier-Smith, I. D. Leroux, and V. Vuletić, Erratum: Squeezing the collective spin of a dilute atomic ensemble by cavity feedback [Phys. Rev. A **81**, 021804(R) (2010)], Phys. Rev. A **83**, 039907(E) (2011).
- [38] H. Bao, J. Duan, S. Jin, X. Lu, P. Li, W. Qu, M. Wang, I. Novikova, E. E. Mikhailov, K.-F. Zhao, K. Mølmer, H. Shen, and Y. Xiao, Spin squeezing of 1011 atoms by prediction and retrodiction measurements, Nature (London) 581, 159 (2020).
- [39] Z. Chen, J. G. Bohnet, S. R. Sankar, J. Dai, and J. K. Thompson, Conditional spin squeezing of a large ensemble

- via the vacuum Rabi splitting, Phys. Rev. Lett. **106**, 133601 (2011).
- [40] O. Hosten, R. Krishnakumar, N. J. Engelsen, and M. A. Kasevich, Quantum phase magnification, Science 352, 1552 (2016).
- [41] D. Linnemann, H. Strobel, W. Muessel, J. Schulz, R. J. Lewis-Swan, K. V. Kheruntsyan, and M. K. Oberthaler, Quantum-enhanced sensing based on time reversal of nonlinear dynamics, Phys. Rev. Lett. 117, 013001 (2016).
- [42] S. Colombo, E. Pedrozo-Peñafiel, A. F. Adiyatullin, Z. Li, E. Mendez, C. Shu, and V. Vuletić, Time-reversal-based quantum metrology with many-body entangled states, Nat. Phys. 18, 925 (2022).
- [43] Z. Li, S. Colombo, C. Shu, G. Velez, S. Pilatowsky-Cameo, R. Schmied, S. Choi, M. Lukin, E. Pedrozo-Peñafiel, and V. Vuletić, Improving metrology with quantum scrambling, Science 380, 1381 (2023).
- [44] J. Borregaard, E. J. Davis, G. S. Bentsen, M. H. Schleier-Smith, and A. S. Sørensen, One- and two-axis squeezing of atomic ensembles in optical cavities, New J. Phys. 19, 093021 (2017).
- [45] J. Hu, W. Chen, Z. Vendeiro, A. Urvoy, B. Braverman, and V. Vuletić, Vacuum spin squeezing, Phys. Rev. A 96, 050301(R) (2017).